

Study of microstress state of P91 steel using complementary mechanical Barkhausen, magnetoacoustic emission, and X-ray diffraction techniques

Bolesław Augustyniak; Leszek Piotrowski; Paweł Maciakowski; Marek Chmielewski; Marzena Lech-Grega; Janusz Żelechowski

 Check for updates

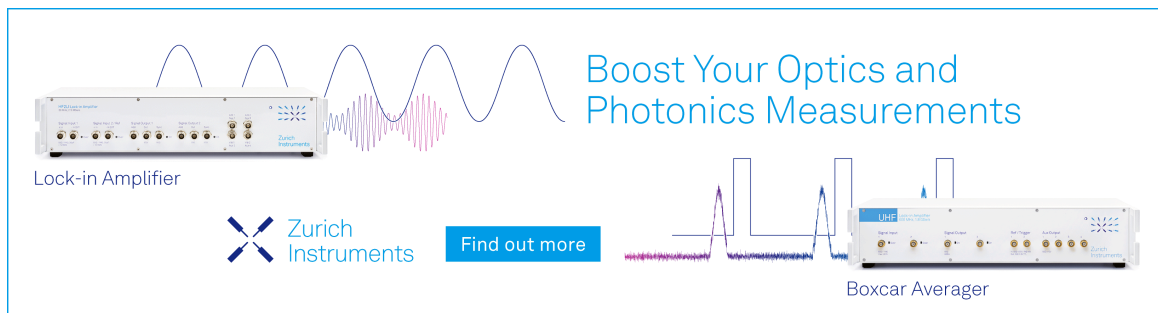
J. Appl. Phys. 115, 17E306 (2014)

<https://doi.org/10.1063/1.4862224>



View
Online


Export
Citation

Boost Your Optics and Photonics Measurements



Lock-in Amplifier

 Zurich Instruments

[Find out more](#)

Boxcar Averager

Study of microstress state of P91 steel using complementary mechanical Barkhausen, magnetoacoustic emission, and X-ray diffraction techniques

Bolesław Augustyniak,^{1,a)} Leszek Piotrowski,¹ Paweł Maciakowski,¹ Marek Chmielewski,¹ Marzena Lech-Grega,² and Janusz Żelechowski²

¹*Faculty of Applied Physics and Mathematics, Gdansk University of Technology, 80-233 Gdansk, Poland*

²*The Institute of Non-Ferrous Metals, 32-050 Skawina, Poland*

(Presented 5 November 2013; received 20 September 2013; accepted 21 October 2013; published online 23 January 2014)

The paper deals with assessment of microstress state of martensite P91 steel using three complementary techniques: mechanical Barkhausen emission, magnetoacoustic emission (MAE), and X-ray diffraction (XRD) profile analysis. Magnetic coercivity H_c and microstructure were investigated with inductive magnetometry and magnetic force microscopy (MFM), respectively. Internal stress level of P91 steel was modified by heat treatment. Steel samples were austenitized, quenched, and then tempered at three temperatures (720 °C, 750 °C, and 780 °C) during increasing time (from 15 min up to 240 min). The microstrain level ε_i was evaluated using Williamson–Hall method. It was revealed that during tempering microstrain systematically decreases from $\varepsilon_i = 2.5 \times 10^{-3}$ for as quenched state down to $\varepsilon_i = 0.3 \times 10^{-3}$ for well tempered samples. Both mechanical hardness (Vicker's HV) and magnetic hardness (coercivity) decrease almost linearly with decreasing microstrain while the MAE and MBE intensities strongly increase. Tempering leads to evident shift of the MeBN intensity maximum recorded for the first load towards lower applied strain values and to increase of MAE intensity. This indicates that the microstress state deduced by magnetic techniques is correlated with microstrains evaluated with XRD technique. © 2014 AIP Publishing LLC. [<http://dx.doi.org/10.1063/1.4862224>]

I. INTRODUCTION

Residual stress, often found in industrial components, may be a cause of serious and costly failure. Unfortunately, assessment of its magnitude is not an easy task, especially in the industrial environment. In this paper, we present the results of multitechnique study of the changes in the residual stress level in P91 grade steel samples subjected to austenitisation process followed by tempering. We compare microstrain level deduced from X-ray profile analysis (Williamson-Hall method WH) width and magnetic hardness measurements (coercivity) as well as with the results of investigation with the help two magnetoelastic effects—mechanical Barkhausen effect (MeBN) and magnetoacoustic emission (MAE). Mechanical Barkhausen effect is a mechanical analogue of classical Barkhausen effect (BE) as both are due to the abrupt, non-continuous motion of magnetic domain walls (DW) and can be detected with the help of a detecting coil placed close to the material surface. The difference is that the BE is caused by the motion of DWs driven by magnetic field while in the MeBN it is caused by the mechanical load.¹ Magnetoacoustic emission is on the other hand an acoustic effect (it consists of acoustic pulses) caused by magnetic field induced abrupt movement of DWs. Both MeBN and MAE are due to the moment of non-90° DWs, as only those are stress sensitive, and can be observed in materials with non-zero magnetostriction.²

II. EXPERIMENTAL

The set of 16 samples made of P91 steel was investigated, and they were austenitized for 1 h at the temperature of 1050 °C and then air quenched. One sample was left in the as quenched state and the remaining 15 samples underwent tempering at three different temperatures (720 °C, 750 °C, and 780 °C) and of various durations (15, 30, 60, 120, and 240 min).

The x-ray diffraction (XRD) measurements were performed with the help of D8-Advance diffractometer (Bruker) in the Bragg-Brentano configuration equipped with Cu anode lamp. The $\text{CuK}\alpha_1$ and $\text{CuK}\alpha_2$ components have been separated with the help of mathematical modelling and the $\text{CuK}\alpha_1$ line was taken into account. Prior to X-ray analysis, the materials were electrochemically polished to relieve deformation zones in the surface. Mechanical Barkhausen noise was measured in a bending mode of deformation with the help of freely vibrating apparatus described in detail elsewhere.³ In this system, the normal mode of oscillations is induced by application of magnetic pull exerted on ferromagnetic rod mounted on the extension arm clamping the sample. Magnetoacoustic emission was measured with the piezoelectric transducer acoustically coupled to the surface of the samples magnetized with the help of encircling coil and a C-core closing the magnetic flux path (details of the set-up can be found in a previous paper⁴). Intensity of the mechanical Barkhausen noise and of magnetoacoustic emission (Ua) are evaluated as rms (root mean square) levels of their input noise like voltage signals. They are plotted as “envelopes” in function of applied strain (ε) and of voltage

^{a)}Author to whom correspondence should be addressed. Electronic mail: bolelek@mif.pg.gda.pl.

U_g proportional to solenoid current intensity, respectively. Magnetic hysteresis loops (necessary to determine coercivity) were recorded in the same magnetizing configuration. Mechanical hardness was measured with standard Vicker's system machine with 30 kG force. Magnetic force microscope images have been obtained measuring phase shift between force and deformation of vibrating probe.

III. RESULTS

It was recognized very early in XRD research that diffraction profile line width is caused by two main effects: (1) the so called size broadening (influence of small crystallite size) and (2) the deformation (strain ϵ) broadening. The latter is often related to dislocations causing extended displacement fields in the crystal. The relative importance of both effects is usually estimated in terms of WH plots—integral peak breadth β vs. $\sin \theta$, where θ is angle of diffraction maximum.⁵ The WH plot can be reformulated in terms of magnitude of diffraction vector $K = 2 \sin \theta / \lambda$ by linear function $dK = \alpha + \epsilon_i K$, where ϵ_i denotes internal strain.⁶ This is valid assuming that peak breadth $\beta = 2\Delta\theta$. It means that microstrain level can be evaluated by means of the slope of the plot dK versus K . The dK is estimated directly from FWHM (full width half maximum). Five diffraction lines corresponding to atomic constant d_{hkl} of ferrite phase defined by hkl indexes equal to $\{110\}$, $\{110\}$, $\{200\}$, $\{211\}$, $\{220\}$, and $\{310\}$ were recorded. It was revealed that dK values corresponding to lines (200) and (310) are systematically shifted up from the regression line (such effect has been already observed⁷). This systematic broadening is due to difference in value of dislocation contrast factor C , which depends on relative orientation between Burgers vector and dislocation line, is probably due to large isotropic deformation in the tested material. Linear approximation of all five dK values gives thus higher level of the internal strain and relatively low correlation factor. Being so we decided to approximate data obtained for three lines: $\{110\}$, $\{211\}$, and $\{220\}$. The results of that analysis are shown in Fig. 1. The strain level ϵ_i for the as-quenched sample (given in the left upper corner of Fig. 1) is very high—over 2500×10^{-6} . As can be seen for all the temperatures the micro strain level systematically decreases, and as it could be predicted the decrease is most pronounced for the highest (780°C) temperature (it decreases down to less than 300×10^{-6}). The observed decrease is due to substantial decrease in dislocation density that takes place during tempering of martensitic steels.⁷ The results of the MAE measurements are shown in Fig. 2—it presents the MAE signal envelopes for samples tempered at 750°C . As it can be seen the MAE signal intensity (that can be characterized by the area under MAE envelopes after subtraction of the noise level⁴) increases significantly as a result of tempering. It is caused by the fact that DW jumps become easier as the dislocation density decreases. Analogous behaviour is observed for the samples tempered at 720°C and 780°C , though for the latter ones the increase is stopped after 120 min—probably due to the ongoing increase in precipitate diameter which grow to the size enabling effective DW pinning. In Fig. 3, there are shown the results of MeBN signal measurements for the “first load,” i.e., for strain increasing

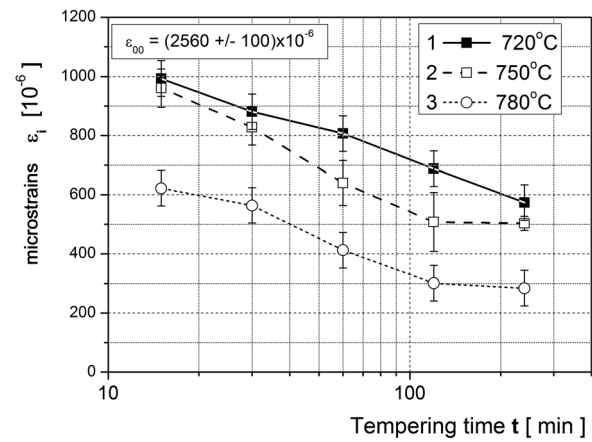


FIG. 1. Internal strain levels for the tested samples evaluated with the help of WH method, plotted in function of tempering time (min).

from initially unstrained, demagnetised sample—the plots show MeBN signal envelopes obtained for the increasing compressive strain. The MeBN intensity was normalized by taking into account deformation velocity changes during sinusoidal oscillations. One can observe that similarly to the results obtained for the MAE signal the overall MeBN intensity increases as a function of tempering time. We assume the envelope of the MBE signal to be strictly related (proportional as a first approximation) to the internal strain distribution function.⁸ This allows one to determine its mean value provided that the applied strain is high enough. Unfortunately, due to very high level of internal stress in martensitic steels, it was not the case for the tested samples. Being so, the position of the envelope maximum was determined (ϵ_{pp}) as, assuming the similar stress distribution function for all the samples, it is correlated with the average internal strain level. The peak position was evaluated with help of data fitting function analysis. Peak position detection was impossible to do so for the as-quenched sample since the MeBN signal was too weak in the available applied strain range. For the rest of the samples the ϵ_{pp} systematically decreases during tempering and the higher the temperature the faster the decrease. The only exception to this rule is the sample tempered at 780°C for

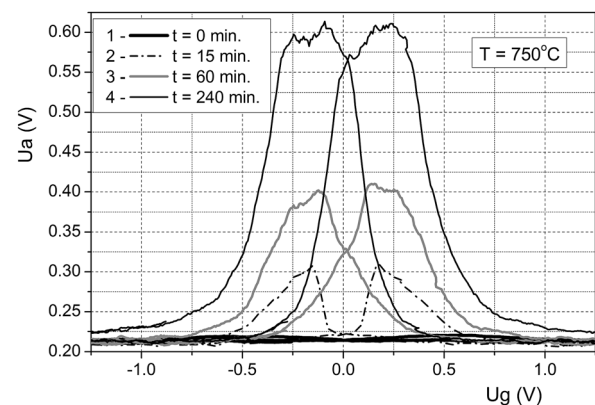


FIG. 2. MAE signal envelopes (U_a) for selected samples tempered at $T = 750^\circ\text{C}$.

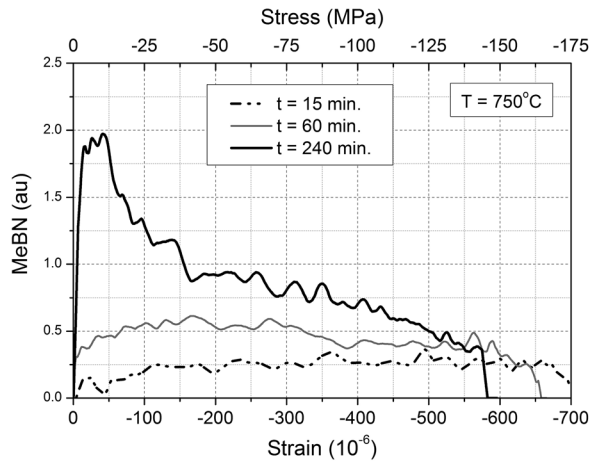


FIG. 3. MeBN signal envelopes obtained for the first load (compressive strains) for selected samples tempered at $T = 750^\circ\text{C}$.

240 min, in which precipitate caused pinning of DW may interfere. Similar behaviour was observed for the magnetic hardness of the investigated samples, i.e., systematic decrease (temperature dependent) of the coercivity, with the exception of the overtempered sample. In order to assess the possibility of internal stress level determination with the applied techniques the correlation plots were drawn in Fig. 4. Plot (1) shows the correlation between the ε_{pp} and the internal strain level ε_i determined with the WH method. As can be seen the correlation is almost linear (both values are proportional), the ε_{pp} values being lower than strain level, what can be explained by the fact that the internal strain distribution function is non-symmetrical (its mean value shifted to higher values relative to its maximum). To some extent, the similar situation takes place for coercivity values (plot (2)); in this case, however, one cannot expect the coercivity to decrease to zero for very low internal strain values since it is caused by pinning on both deformation fields (dislocation tangles) and precipitates (always present in steels). Only the first mechanism is dependent on dislocation density and hence internal strain level. As for the MAE signal intensity (plot (3)), the correlation is

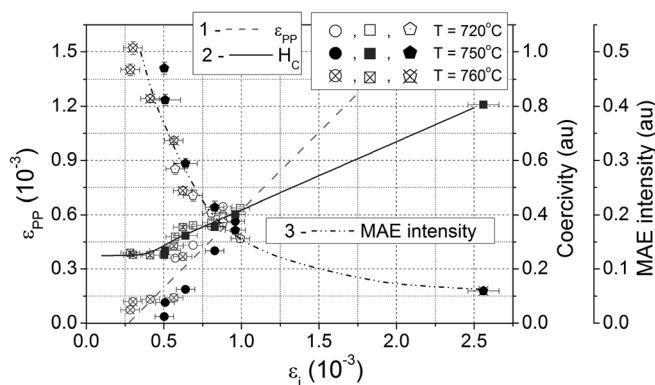


FIG. 4. Correlations between internal stress level ε_i and the investigated parameters: 1—MeBN envelope peak position ε_{pp} , 2—coercivity related to not tempered state, and 3—MAE intensity.

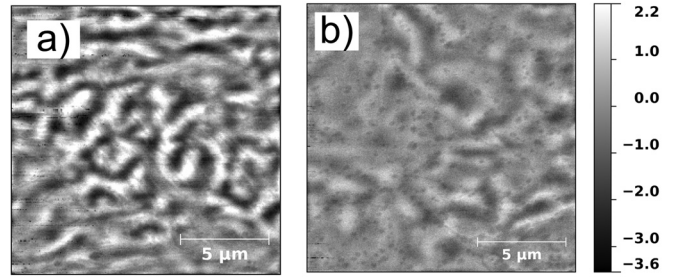


FIG. 5. MFM images obtained for the as quenched (a) and tempered ($T = 750^\circ$, $t = 240$ min) sample (b).

strongly nonlinear for higher strain values; yet in the whole range of investigated deformations, it is monotonous allowing for the non ambiguous determination of internal stress level.

The as described magnetoelastic techniques confirm the XRD results suggesting significant decrease of strain fields intensity. Further evidenced is given by a direct observation of magnetic surface domains, stray fields observed for the as quenched sample (Fig. 5(a)) are significantly higher than for the sample tempered for 240 min at 750°C (Fig. 5(b)). Such decrease suggests much lower strain induced anisotropy of the tempered sample.

IV. CONCLUSIONS

We argue that our results make evident that all the described techniques are potentially useful for evaluation of the internal microstress level in ferromagnetic material. We look, however, for techniques which can be useful for industrial application when steel microstructure state is in question. The most direct correlation with microstrain level is observed for the peak position of Mechanical Barkhausen effect intensity; yet, such measurements can be performed only in laboratory conditions. Coercivity level can be estimated indirectly with the help of an external electromagnet; yet, such magnetisation leads to much lower sensitivity. The MAE effect intensity—also very sensitive to microstrain level—seems to be the most promising for application in industrial environment. To our best knowledge, it is the first time that a direct correlation between microstrain level, determined with the help of WH method, and magnetomechanical properties is proved.

¹B. Augustyniak, P. Maciakowski, L. Piotrowski, and M. Chmielewski, *IEEE Trans. Magn.* **48**, 1405 (2012).

²B. Augustyniak, M. J. Sablik, F. J. G. Landgraf, D. C. Jiles, M. Chmielewski, L. Piotrowski, and A. J. Moses, *J. Magn. Magn. Mater.* **320**, 2530 (2008).

³P. Maciakowski, B. Augustyniak, M. Chmielewski, and L. Piotrowski, *J. Electr. Eng.* **63/7s**, 102 (2012).

⁴L. Piotrowski, B. Augustyniak, M. Chmielewski, F. J. G. Landgraf, and M. J. Sablik, *NDT&E Int.* **42**, 92 (2009).

⁵G. K. Williamson and W. H. Hall, *Acta Metall.* **1**, 22 (1953).

⁶S. Takebayashi, T. Kuneida, N. Yosinaga, K. Ushioda, and S. Ogata, *ISIJ Int.* **50**, 875 (2010).

⁷J. Pesicka, R. Kuzel, A. Dronhofer, and G. Eggeler, *Acta Mater.* **51**, 4847 (2003).

⁸B. Augustyniak and J. Degauque, *J. Phys.* **6(8)**, C-527 (1996).